STUDY OF DUCTILITY EVALUATIONS ON REINFORCED CONCRETE COLUMNS SUBJECTED TO REVERSED CYCLIC LOADING WITH LARGE DEFORMATIONS

(Translation from Proceedings of JSCE, No.711/V-56, August 2002)





Tadayoshi ISHIBASHI Takeshi TSUYOSHI Kaoru KOBAYASHI Toru YOSHIDA Takuya UMIHARA

The level of damage to the reinforced concrete members that comprise a structure can be used as an index of the structure's seismic performance. The rational seismic-resistant design of structures therefore requires a suitable method of evaluating the relationship between plastic deformation and level of damage. Further, it is necessary to obtain a quantitative evaluation of ductility, which represents the level of damage. To this end, the authors carry out reversed cyclic loading tests on model RC columns with large deformational capacity and examine the influence of the major parameters on their deformation capacity. This paper reports the resulting quantitative evaluation of the ductility of RC column members.

Keywords: *reinforced concrete column, ductility, seismic resistant design, reversed cyclic loading*

Tadayoshi Ishibashi is a manager in the Structural Engineering Center of the Construction Department of East Japan Railway Company. He obtained his D.Eng from the University of Tokyo in 1983. His research interests relate to the seismic design of concrete structures for railways. He is a Fellow of JSCE.

Takeshi Tsuyoshi is a group leader in the Tokaido Sobu Department at the Tokyo Construction Office of East Japan Railway Company. He obtained his D.Eng from the University of Tokyo in 2001. His research interests relate to the seismic design of concrete structures for railways. He is a member of JSCE.

Kaoru Kobayashi is a group leader at the Research & Development Center of East Japan Railway Company. He obtained his D.Eng from the University of Tokyo in 2001. His research interests relate to the seismic design of concrete structures for railways. He is a member of JSCE.

Toru Yoshida is a member of the Structural Engineering Center of the Construction Department of East Japan Railway Company. His research interests relate to the seismic design of concrete structures for railways. He is a member of JSCE.

Takuya Umihara is the member of the Construction Division of the Engineering Department at Hokkaido Railway Campany. His research interests relate to the seismic design of concrete structures for railways. He is a member of JSCE.

1. Introduction

The aseismic performance of reinforced concrete (RC) structures is measured in terms of the ease/difficulty with which they can be restored after an earthquake [1], [2], and this is closely related to the damage suffered by structural members. Consequently, rational aseismic design depends on clarifying the relationship between plastic deformation and the level of damage to members, and assessing their deformational capacity at different damage levels.

In view of the damage caused by the Hyogo-ken Nambu (Southern Hyogo) Earthquake, it has become necessary to greatly improve the aseismic performance of RC structures. This requires assessment of the aseismic performance of RC members in the region of large deformation, or at about 10 times the yield displacement [1]. However, the behavior of RC columns at extreme deformations, such as beyond the maximum strength, has not been sufficiently clarified as yet.

To evaluate damage levels and their correlation with the degree of plastic deformation [3], the authors have previously performed reversed cyclic loading tests on RC columns modeled on those of a rigid-frame railway bridge in the region of large deformation, at a ductility factor of 10 [3]. A method of calculating the degree of pull-out of the axial reinforcement in the large deformation area has also been proposed [4].

In this paper, the authors discuss the factors that influence the deformation capacity of model RC specimens with a dense arrangement of hoop reinforcement based on reversed cyclic loading tests. A method is proposed for calculating the deformation capacity of an RC column at a ductility factor as high as 10.

2. Outline of reversed cyclic loading tests

(1) Specimen dimensions

Table 1, Fig. 1, and Table 2 show the dimensions of a specimen, a typical reinforcing bar arrangement, and the results of material strength tests, respectively. The specimen cross section was generally about half that of a rigid-frame railway viaduct column. The web reinforcement ratio (pw) was 0.6% or more in most of the specimens. Other parameters were the shear span ratio (a/d), tensile reinforcement ratio (pt = ΣAs/(B·d), where ΣAs is the total area of axial reinforcement at the outermost edge of the tension side; B is the column section width; and d is the effective column height), and axial compressive stress (σ_{n0}). The actual value of strength obtained from material strength tests was used to calculate the strength ratio (Vy/Vmu, where Vy is the shear strength of the member; Vmu = Mu/a; Mu is the flexural strength; and a is the shear span) given in Table 1 [5]. To calculate the shear strength (Vc) of linear members without shear reinforcement, we used an expression proposed by Niwa et al. [6] and Ishibashi et al. [7] that reflects the effects of a/d.

(2) Loading method

Figure 2 shows the configuration for reversed cyclic loading tests. An axial force (axial compressive stress of 0.49N/mm^2 to 5.88N/mm^2) was applied using a vertical jack, with each specimen consisting of a column and its footing attached to the floor with PC steel bars.

Horizontal loading was then applied with an actuator near the column head by means of load control in both positive and negative direction until the reading of a strain gage pasted to an axial reinforcement bar at the column foot exceeded the yield strain as obtained in tensile tests of the reinforcement. The horizontal displacement at the horizontal loading point was taken as the measured reference yield displacement (δytest),

Table 1 Dimensions of specimen

Specimen No	Height of cross section h (mm)	Width of cross section b (mm)	Cover c (mm)	Effective height d (mm)	Shear span a (mm)	Shear span ratio a/d	Tensile reinforcement			Side tensile reinforcement		Hoop reinforcement			Axial compressive stress σ 'no (N/mm2)	Strength ratio Vy/Vmu	Loading pattern
							Diameter	Quantity (pieces)	Reinforcement ratio pt (%)	Diameter	Quantity (one side) (pieces)	Diameter	Span (mm)	Reinforcement ratio pw (%)			
No2	400	400	40	360	1150	3.19	D19	5	0.995	D19	3	D13	70	0.905	0.98	2.26	A
No4	400	400	40	360	1150	3.19	D16	5	0.690	D16	3	D13	90	0.704	0.49	2.46	A
A1	400	400	40	360	1150	3.19	D19	5	0.995	D19	3	D13	80	0.792	0.98	2.05	B
A2	400	400	40	360	1150	3.19	D19	5	0.995	D19	3	D13	60	1.056	0.98	2.52	B
A3	400	400	40	360	1150	3.19	D16	5	0.690	D16	3	D13	70	0.905	0.49	2.94	B
A4	400	400	40	360	1150	3.19	D13	5	0.440	D13	3	D13	80	0.792	0.98	3.86	B
A5	400	400	40	360	1150	3.19	D13	5	0.440	D13	3	D13	140	0.453	0.98	2.66	B
A6	400	400	40	360	1150	3.19	D19	5	0.995	D19	3	D13	50	1.267	0.98	2.87	B
A7	400	400	40	360	1150	3.19	D19	5	0.995	D19	3	D13	60	1.056	0.98	2.51	A
A8	400	400	40	360	1150	3.19	D16	5	0.690	D16	3	D13	120	0.528	0.98	1.98	B
A9	400	400	40	360	1150	3.19	D19	5	0.995	D19	3	D16	60	1.655	0.98	3.94	B
A10	700	400	40	660	1000	1.52	D19	5	0.543	D19	4	D13	60	1.056	0.98	2.01	B
A11	500	500	40	460	1150	2.50	D19	5	0.623	D19	3	D13	60	0.845	0.98	2.36	B
K1	400	400	40	360	1150	3.19	D19	5	0.995	D19	3	D13	65	1.056	0.98	2.56	B
R1	400	400	40	360	1150	3.19	D19	5	0.995	D19	3	D13	70	0.905	2.94	1.96	B
R2	400	400	40	360	1150	3.19	D19	5	0.995	D19	3	D13	60	1.056	5.88	2.04	B
R3	400	400	40	360	1150	3.19	D19	5	0.995	D19	3	D13	80	0.792	0.98	1.90	A
R4	400	400	40	360	1150	3.19	D19	5	0.995	D19	3	D13	70	0.905	2.94	1.94	A

Table 2 Results of material strength tests

Specimen No	Strength of concrete		Axial reinforcement				Hoop
	Column (N/mm^2)	Footing (N/mm^2)	Yield strength (N/mm^2)	Tensile strength (N/mm^2)	Yield strain $\varepsilon y \times 10^{-6}$	Strain hardening initiation point ε sh ×10-6	Yield strength (N/mm^2)
No2	23.5	28.2	378.5	543.0	2068	18409	359.3
No4	28.2	24.3	397.5	556.5	2153	19341	359.3
A1	26.4	31.4	378.6	543.0	2069	18920	358.5
A2	23.3	29.0	378.6	543.0	2069	18920	358.5
A3	26.8	24.8	397.5	556.5	2156	20449	358.5
A4	28.4	27.6	358.5	514.7	1980	19459	358.5
A5	29.1	29.4	358.5	514.7	1980	19459	358.5
A6	30.9	28.6	378.6	543.0	2069	18920	358.5
A7	30.7	30.3	378.6	543.0	2069	18920	358.5
A8	23.8	30.0	397.5	556.5	2156	20449	358.5
A9	21.7	22.2	378.6	543.0	2069	18920	397.5
A10	22.4	21.8	378.6	543.0	2069	18920	358.5
A11	24.6	24.4	378.6	543.0	2069	18920	358.5
K1	19.4	19.6	375.4	554.2	2061	18689	358.5
R1	28.2	30.4	389.5	587.8	2339	13914	368.2
R2	30.8	34.7	389.5	587.8	2339	13914	368.2
R3	32.5	32.3	389.5	587.8	2339	13914	368.2
R4	35.2	36.2	389.5	587.8	2339	13914	368.2

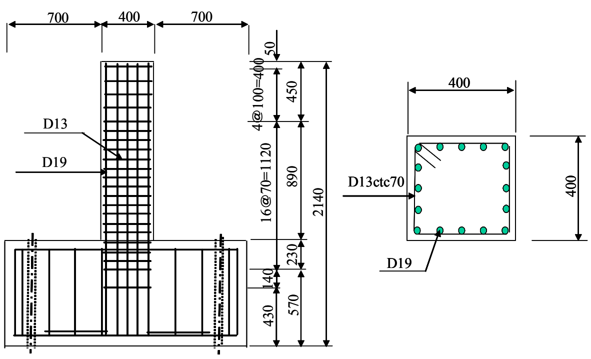

Fig. 1 Example of bar arrangement (specimen No. 2)

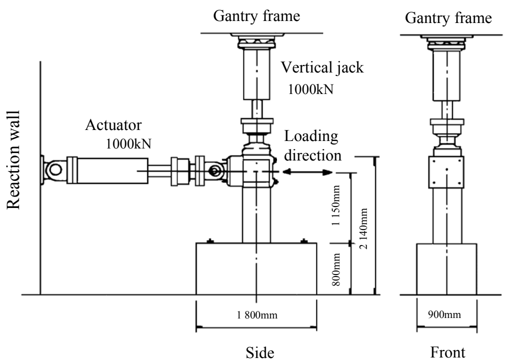

Fig. 2 Configuration of reversed cyclic loading tests

Table 3 Summary of test and calculation results

Specimen No	δy'test	δy1	δy0	δycal	δmtest	δm1	δmb	δmp	φpmtest	φpmcal	δmcal	δutest	δu1	δub	δup	φputest	φpucal	δucal
No2	5.23	1.83	3.66	5.49	59.31	12.11	1.24	45.96	0.000152	0.000140	55.79	70.43	15.44	0.95	54.04	0.000179	0.000184	72.23
No4	4.17	1.56	3.68	5.24	36.70	7.68	1.28	27.75	0.000092	0.000122	45.78	60.47	11.70	0.97	47.81	0.000158	0.000171	64.50
A1	6.28	1.68	3.59	5.27	62.40	11.75	1.22	49.44	0.000163	0.000130	52.42	75.04	14.85	0.93	59.26	0.000196	0.000177	69.49
A2	6.68	1.81	3.67	5.48	73.47	13.59	1.24	58.64	0.000194	0.000152	60.71	84.19	17.05	0.95	66.19	0.000219	0.000193	76.30
A3	5.50	1.56	3.48	5.04	57.04	9.67	1.21	46.16	0.000153	0.000140	53.32	78.19	13.85	0.90	63.45	0.000210	0.000184	70.59
A4	3.12	0.93	2.80	3.73	46.72	7.94	0.90	37.88	0.000125	0.000130	48.30	77.10	10.02	0.60	66.48	0.000220	0.000177	64.33
A5	2.94	0.88	2.79	3.67	39.05	6.56	0.90	31.59	0.000104	0.000089	34.42	56.93	9.56	0.60	46.76	0.000155	0.000148	54.95
A6	5.41	1.73	3.48	5.21	76.04	13.93	1.19	60.92	0.000201	0.000165	65.07	94.27	16.28	0.90	77.09	0.000255	0.000202	78.39
A7	5.50	1.67	3.49	5.16	48.81	9.22	1.19	38.40	0.000127	0.000152	56.29	71.37	13.85	0.90	56.62	0.000187	0.000193	73.05
A8	4.28	1.44	3.59	5.03	50.10	8.14	1.21	40.75	0.000135	0.000100	39.75	65.08	11.25	0.90	52.93	0.000175	0.000156	59.39
A9	5.58	2.19	3.72	5.91	79.47	16.57	1.25	61.65	0.000204	0.000185	73.74	89.57	20.77	0.97	67.83	0.000224	0.000216	87.20
A10	4.11	0.85	1.38	2.23	43.57	9.26	0.03	34.29	0.000084	0.000072	38.80	47.99	8.76	0.02	39.21	0.000096	0.000091	46.28
A11	5.68	1.34	2.60	3.94	53.28	10.85	0.55	41.88	0.000115	0.000106	49.90	72.57	13.40	0.40	58.77	0.000161	0.000142	65.32
K1	5.19	2.41	3.77	6.18	63.75	15.52	1.26	46.98	0.000155	0.000152	62.66	78.58	16.45	0.98	61.15	0.000202	0.000193	80.84
R1	5.62	2.33	3.80	6.13	63.97	14.41	1.18	48.38	0.000160	0.000140	58.03	80.45	18.71	0.91	60.83	0.000201	0.000184	75.45
R2	5.88	2.35	3.97	6.32	61.02	13.73	1.07	46.22	0.000153	0.000152	60.68	81.66	18.07	0.88	62.71	0.000207	0.000193	77.25
R3	4.90	2.01	3.55	5.56	52.44	11.25	1.22	39.97	0.000132	0.000130	51.93	62.47	13.50	0.92	48.05	0.000159	0.000177	68.13
R4	5.41	1.98	3.60	5.58	59.14	11.06	1.14	46.94	0.000155	0.000140	54.64	68.01	14.52	0.86	52.63	0.000174	0.000184	71.22

δy'test: Measured yield displacement (mm), δy1: Rotational displacement due to pull-out of axial reinforcement at yield displacement (mm), δy0: Displacement of the skeleton at the yield displacement (mm), δycal: Calculated yield displacement (mm), δmtest: Measured maximum displacement to maintain maximum load (mm), δm1: Rotational displacement due to pull-out of axial reinforcement at the maximum displacement to maintain the maximum load (mm), δmb: Displacement of skeleton away from plastic-hinge at maximum displacement to maintain maximum load (mm), δmp: Displacement due to rotation of plastic hinge at maximum displacement to maintain maximum load (mm),
φpmtest: Measured average curvature of plastic hinge at maximum displacement to maintain maximum load (1/mm), φpmcal, Calculated average curvature of plastic hinge at maximum displacement to maintain maximum load (1/mm), δmcal: Calculated maximum displacement to maintain maximum load (mm), δutest: Measured ultimate displacement (mm), δu1: Rotational displacement due to pull-out of axial reinforcement at ultimate displacement (mm), δub: Displacement of skeleton away from plastic-hinge at ultimate displacement (mm), δup: Displacement due to rotation of plastic hinge at ultimate displacement (mm), φputest: Measured average curvature of plastic hinge at ultimate displacement (1/mm), φpucal: Measured average curvature of plastic hinge at ultimate displacement (1/mm), δucal: Calculated ultimate displacement (mm)

while the vertical load was taken to be the measured yield load (Pytest) at the point when the axial reinforcement at the outermost edge reached the yield strain.

After the specimen yielded, reversed cyclic loading was applied in the horizontal direction by means of displacement control. Reversed loads were applied at even multiples of δytest with one cycle in each of the positive and negative directions first, and then at integer multiples of δytest with on cycle in each direction once the horizontal load began decreasing under loading pattern A in Table 1. In the case of loading pattern B, loading was at integer multiples of δytest with one cycle in each direction once the horizontal load began to decrease. Loading pattern A was used in the initial stage of the tests. At large displacements beyond 10·δytest, however, the axial reinforcement yielded after few cycles and this governed the deformation capacity of the specimen. Failures of this type have rarely been recognized during actual earthquakes, and other researchers have also pointed out that the possibility of such failure is very small [8]. Since the purpose of these tests was to evaluate deformation capacity in the absence of reinforcement failure, it was decided to adopt loading pattern B to avoid fatigue failure of the axial reinforcement.

3. Load-displacement relationship in reversed cyclic loading tests

(1) Load-displacement curve

Figure 3 shows a typical load-displacement curve obtained in the tests. The load-displacement envelope reaches a maximum load at a displacement equivalent to about twice the yield displacement. Thereafter, the horizontal load remains approximately constant until the displacement reaches about 80% of the ultimate displacement (the lateral maximum displacement on the envelope of the load-displacement curve where load falls to the calculated yield load) with all specimens.

Table 3 summarizes the test results. Here, the measured value of yield displacement (δy'test) is the horizontal displacement corresponding to the calculated yield load (Pycal). The effect of P - δ due to axial force is taken into account in evaluating loads in this study

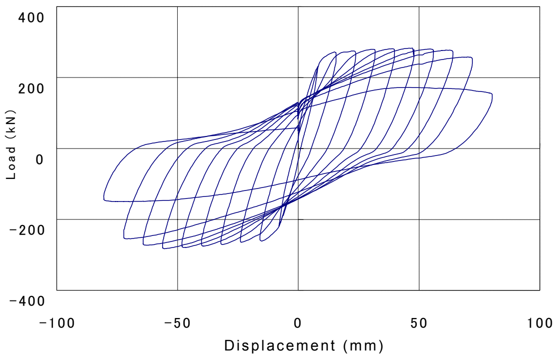

Fig. 3 Typical load-displacement curve (specimen A1)

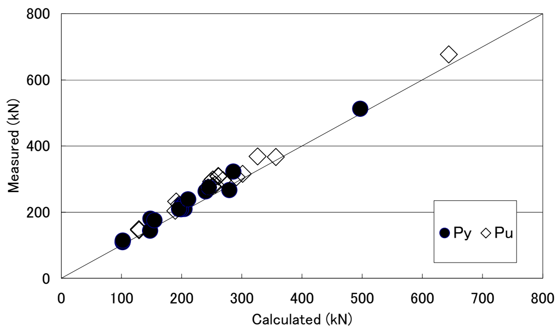

Fig. 4 Relationship between measured and calculated loads

[9].

(2) Yield and maximum loads

Figure 4 shows the relationships between measured and calculated yield load (Py) and the maximum load (Pu). The calculated yield load (Pycal) is defined as the load at the horizontal loading point when the axial reinforcement at the outermost tension edge reaches the yield strength, as in most past studies (such as references [3], [4] and [10]). The maximum load (Pucal) was calculated at the concrete ultimate strain of 0.0035, according to the Standard Specifications for Design of Concrete Structures for Railways [5]. Values obtained from material strength tests were used to calculate the yield strength of the reinforcement and the compressive stress of the concrete.

From Fig. 4, it is inferred that the calculated values of load approximately reflect the measured values.

(3) Effect of various factors on load-displacement envelope

All of the RC specimens tested in this study underwent flexural failure (with flaking and gradual pulverization of the concrete cover on the loading plane, followed by loss of strength after yielding of the axial reinforcement, before eventually reaching the ultimate state).

The effects of several variables on the load-displacement curves obtained in the tests are summarized here. Since each specimen had a different yield load due to variations in these factors, the Y-axis in the figures given in this section represents a non-dimensional value obtained by dividing the horizontal load by the calculated yield load (Pycal).

a) Effect of web reinforcement ratio
Figure 5 shows the load-displacement envelopes for three specimens with different web reinforcement ratios, A1 (0.792%), A2 (1.056%), and A3 (1.655%) and a tensile reinforcement ratio of 0.995. Axial compressive stress was 0.98N/mm^2 and all specimens were subjected to the same reversed cyclic loading pattern. The ultimate displacement is clearly larger at higher web reinforcement ratios.

b) Effect of axial compressive stress
Figure 6 shows load-displacement envelopes for three specimens, K1, R1, and R2, with a tensile reinforcement ratio of 0.995% and a strength ratio of about 2.0 under axial compressive stresses of 0.98N/mm^2, 2.94N/mm^2, and 5.88N/mm^2. The same reversed cyclic loading pattern was applied. Within the range of axial compressive stresses tested in this study, ultimate displacement was little affected by variations in axial compressive

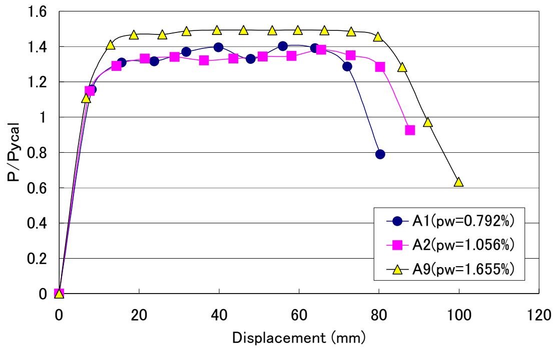

Fig. 5 Envelopes of load-displacement curves
(at different values of pw)

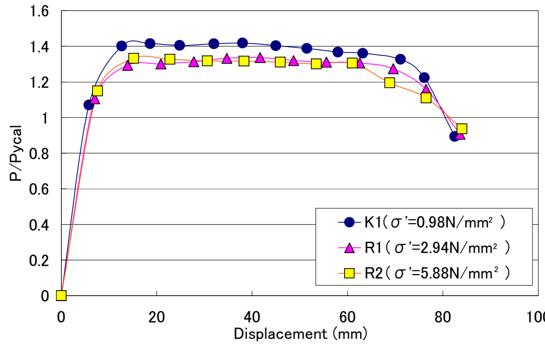

Fig. 6 Envelopes of load-displacement curves
(at different values of σ'_{n0})

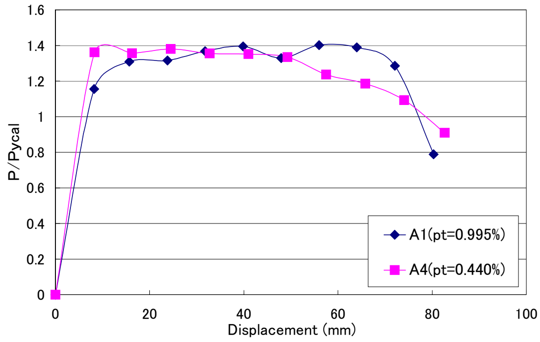

Fig. 7 Envelopes of load-displacement curves
(at different values of pt)

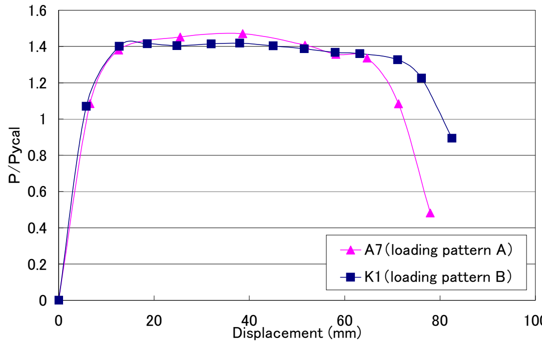

Fig. 8 Envelopes of load-displacement curves
(with different loading patterns)

stress.

c) Effect of tensile reinforcement ratio
Figure 7 shows the load-displacement envelopes for two specimens, A1 and A4, with tensile reinforcement ratios of 0.995% and 0.440%. In this case, the axial compressive stress was 0.98N/mm^2 and the web reinforcement ratio was 0.792%, and the same reversed cyclic loading pattern was applied. Within the range of tensile reinforcement ratios tested in this study, ultimate displacement was little affected by variations in tensile reinforcement ratio.

d) Effect of the frequency of reversed cyclic loading at different displacements
Figure 8 shows the load-displacement envelopes at an axial compressive stress of 0.98N/mm^2, a tensile reinforcement ratio of 0.995%, and a web reinforcement ratio of 1.056% for specimen A7 subjected to three cycles of loading at different displacements under loading pattern A (as explained in section 2.(2) "Loading method") and for specimen K1 subjected to one cycle of loading at different displacements under the loading pattern B. The ultimate displacement of specimen A7 was less than that of specimen K1.

e) Effect of shear span
Figure 9 shows the load-displacement envelopes at an axial compressive stress of 0.98N/mm^2 and a strength ratio of about 2.0 for three specimens under the same reversed cyclic loading pattern: K1 (shear span ratio: 3.19), A11 (2.50), and A10 (1.52). The ultimate displacement tended to decrease as the shear span ratio decreased.

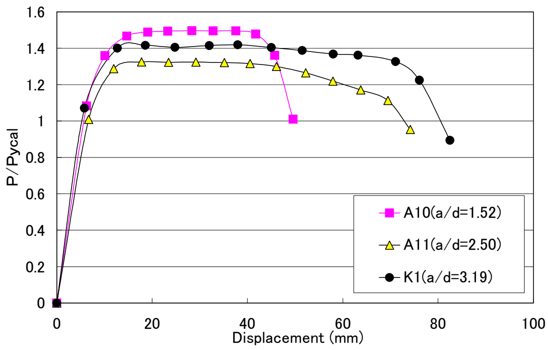

Fig. 9 Envelopes of load-displacement curves (at different values of a/d)

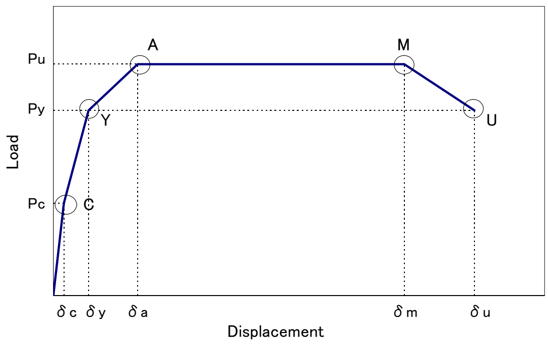

Fig. 10 Modeled skeleton curve

4. Deformation capacity of RC columns subjected to reversed cyclic loading

(1) Modeling of skeleton curve

Figure 10 shows a skeleton curve modeled on the basis of the load-displacement curves obtained from the reversed cyclic loading tests. In this modeled curve, C is the point where flexural cracking occurs; Y is the yield point (where the outermost axial reinforcement reaches the yield strain); A is the approximate point of displacement at which the maximum load is reached after the yield point; and M is the point of maximum displacement where the maximum load is maintained. The authors have confirmed in previous research [3] that cross-sectional damage at point M is limited and restricted to the concrete cover surface layer at the foot of the loading plane, allowing the column to continue in use after simple re-grouting of the cracks. If the damage exceeds this level, flaking of the concrete cover occurs and repair of the cross section is necessary. We define the ultimate point U on the load-displacement envelope as the point of the maximum displacement at which the load reaches the calculated yield load (Pycal). At point U, damage is concentrated at the foot of the member, where the core concrete is pulverized, but strength has not dropped so much that repairs cannot recover performance.

In the same previous work, it was reported that the ratio of loading at point M to the maximum load is about 97%. In evaluating deformation capacity, therefore, we set the displacement at point M on the load-displacement envelope such that 97% of the maximum load is maintained. We also set the displacement at point A such that 97% of the maximum load is reached. The displacement is then about twice the yield displacement in the case of most specimens, though there is a relatively wide variation with displacements ranging from one to four times the yield displacement. The method used to calculate displacement at points Y, M, and U in Fig. 10 is explained below.

(2) Yield displacement (point Y)

The yield displacement of an RC column is the sum of two components, the rotational displacement arising from pull-out of the axial reinforcement from the footing and the displacement of the skeleton. In the following calculations of displacement, therefore, we discuss these two components separately.

a) Rotational displacement
Expression (1) proposed by Shima et al. [11] is used to express the measured pull-out, S, of reinforcement from the footing at yield to quite high precision [4], and this value is substituted into Expression (2) [5] to calculate the equivalent rotational displacement at yield.

$$S = 7.4\alpha_y \cdot \varepsilon y(2 + 3{,}500\varepsilon_y)/(f'_{ck})^{2/3} \cdot \varphi \quad \ldots \quad (1)$$

Where,
S: pull-out of reinforcement (cm)
α_y: effect of bar spacing [12]

$$\alpha y = 1 + 0.9e^{0.45(1 - Cs/\varphi)}$$

Where,
ε_y: strain at reinforcement yield
φ: diameter of reinforcing bars (cm)
f'_{ck}: strength of footing concrete (N/mm^2)
Cs: bar spacing (cm)

$$\delta_1 = a \cdot S/(d - x) \quad \ldots \quad (2)$$

Where,
δ_1: rotational displacement due to pull-out of axial reinforcement
a: shear span or length of member
S: pull-out of reinforcement
d: effective height (height of cross section minus distance from the compression (tension) edge to the compression (tensile) reinforcement at ultimate displacement [4])
x: distance from compression edge to neutral axis (at ultimate displacement ; distance from neutral axis to center of compressive reinforcement [4])

b) Displacement of the skeleton
Displacement of the skeleton at the yield displacement is obtained by dividing the member into 100 segments in the axial direction, and integrating the curvature of all segments. In calculating the curvature, the total cross section is regarded as effective if no cracking occurs in the calculation, while concrete on the tension side is neglected when cracking occurs. Cracking is found to occur when the tensile stress at the concrete edge reaches the flexural strength in consideration of member dimensions [5].

c) Comparison of calculated and measured values of yield displacement
Figure 11 shows the relationship between calculated yield displacement (δycal = δy1 + δy0, where δy1 is the rotational displacement due to the pull-out of axial reinforcement and δy0 is the displacement of the skeleton, both at the yield displacement) and the measured value (δy'test). The calculated values approximately correlate with the measured values.

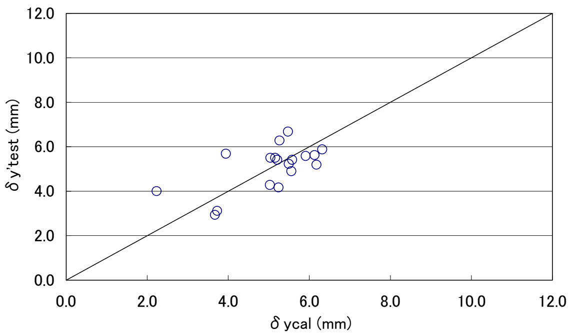

Fig. 11 Comparison of δy'test and δycal

<u>(3) Ultimate displacement (point U)</u>

The ultimate displacement (δu) is the sum of the rotational displacement and the displacement of the skeleton (δu1) at the ultimate state.

a) Rotational displacement arising from pull-out of axial reinforcement
The amount of pull-out S from the footing after yielding of the axial reinforcement is obtained using expressions (3) to (5), and this value is substituted it into Expression (2) to calculate the rotational displacement (δu1) arising as a result of pull-out of the axial reinforcement at the yield displacement.

$$S = s \cdot \varphi / K_{fc} \quad \ldots \quad (3)$$

Where,
S: pull-out of reinforcement (cm)
s: non-dimensional measure of reinforcement pull-out
φ: diameter of reinforcing bar (cm), $K_{fc} = (f_{ck}/20)^{2/3}$
f_{ck}: strength of footing concrete (N/mm^2)

① When the reinforcement strain takes the value of yield strain (εy).
$s = \varepsilon_y(2 + 3{,}500\varepsilon_y)\cdot\alpha_y$
② When the reinforcement strain is at the initiation point of the strain hardening area (εsh).
$s = 0.5(\varepsilon_{sh} - \varepsilon_y) + s(\varepsilon_y)$
③ When the reinforcement strain takes the value at the change in gradient of the non-dimensional slip in the reinforcement strain hardening area.(εa).
$s = 0.08(f_u - f_y)(\varepsilon_a - \varepsilon_{sh}) + s(\varepsilon_{sh})$
④ When the reinforcement strain is greater than ε_a.
$s = 0.027(f_u - f_y)(\varepsilon_s - \varepsilon_a) + s(\varepsilon_a)$
… (4)

Where,
ε_y: strain at reinforcement yield
ε_{sh}: strain at initiation of reinforcement strain hardening
f_u: tensile strength of reinforcement (N/mm^2)
f_y: yield strength of reinforcement (N/mm^2)
εs: reinforcement strain
α_y: effect of bar spacing [12] ($\alpha_y = 1 + 0.9e^{0.45(1 - Cs/\varphi)}$)
C_s: bar spacing (cm)
φ: diameter of reinforcing bar (cm)
ε_a: point of non-dimensional slip gradient change in the strain hardening area
$\varepsilon_a = \varepsilon_{sh} + \{(0.132 - s(\varepsilon_y)/2)/(0.13(f_u - f_y))\}$
$s(\varepsilon_y)$: non-dimensional amount of pull-out at reinforcement yield strain
$s(\varepsilon_{sh})$: non-dimensional amount of pull-out when the reinforcement strain is at the strain hardening starting point
$s(\varepsilon_a)$: non-dimensional amount of pull-out when the reinforcement strain is ε_a.

$\varepsilon = 0.0031\cdot\mu + 0.0099$ … (5)

However, $2 \leqq \mu < 14$
$3.55 \leqq w/\varphi \leqq 7.69$
Where,
ε: reinforcement strain at the footing top
μ: ductility factor of member
w: Bar spacing (cm)
φ: diameter of reinforcing bar (cm)

b) Deformation capacity of skeleton after member yield
Past research [13] indicates that displacement due to rotation within a certain rage at the foot of the member predominates in the overall displacement of the skeleton after a RC column subjected to reversed cyclic loading reaches yield. In the tests carried out here, it was confirmed that damage was concentrated at the foot of the member and that this caused displacement due to rotation around the point at which diagonal cracks intersected. It is thought that displacement of the skeleton was mostly due

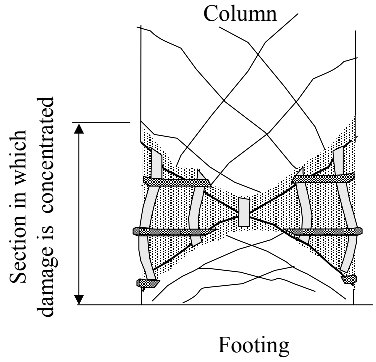

Fig. 12 Conceptual drawing of damage at foot of member

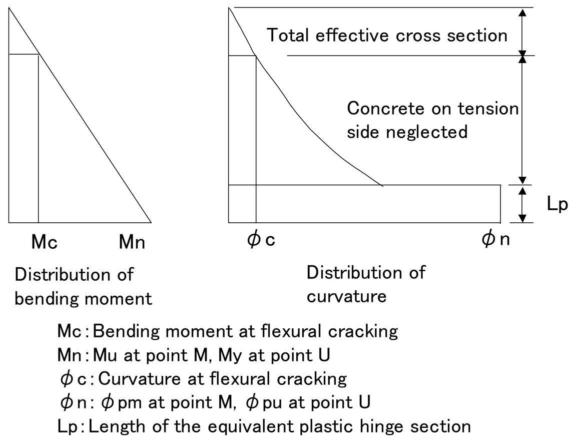

Fig. 13 Schematic drawing of distribution of curvature after yield of member

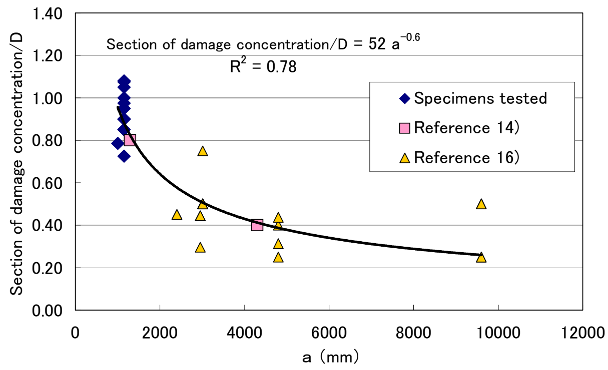

Fig. 14 Relation between a and the section length of damage concentration divided by D

to yield displacement at this point. We define the mechanism by which hinge-like plastic deformation occurs at the end of the member under reversed cyclic loading as a plastic hinge.

We assume a curvature distribution of the RC column after member yield as shown schematically in Fig. 13. It is thought that the curvature distribution is locally dense in the section where the plastic hinge occurs. In order to treat the curvature in this section as constant, we need to define the section in which the plastic hinge occurs and the average curvature in that section in calculating the displacements. In the text that follows, the section in which the plastic hinge occurs is discussed in view of the damage that took place in the reversed cycling tests.

It is reported in the literature [14] that the length-to-height ratio of the area of concentrated damage is less in large specimens than in small specimens, presumably due to the effects of column diameter and hoop dimensions. In another report [15], test results demonstrate that the range of plastic curvature at the column foot is smaller with large specimens than with small specimens, and differences in the length over which the axial reinforcement buckles depending on reinforcement diameter and the span of intermediate hoops are given as the reason for this. However, no method of quantitatively determining the length of the section of concentrated damage is given.

Here, we discuss such a method on the basis of our data as well as the data presented in the literature [14], [15], and [16]. In Fig. 14, the X-axis represents shear span, and the Y-axis is the ratio of the length of the section with concentrated damage after yielding of the member to the section height (D). The figure shows that damage is typically concentrated into a length of about 1.0D for the range of shear spans tested in this study. Also plotted in Fig. 14 are the test results obtained by Kosa et al. [14] and given in a Technical Memorandum of the Public Works Research Institute [16]; these covered larger shear spans. (The data from the latter includes that obtained by Hoshikuma et al. [15].) The concentrated damage length divided by D tends to decreases as the shear span increases. If this portion in which damage is concentrated is taken to be the length of the equivalent plastic hinge Lp, we obtain Expression (6).

$$Lp = 52 \cdot a\text{-}0.6 \cdot D \quad \ldots \quad (6)$$

However, Lp ≦ D
Where,
Lp: length of equivalent plastic hinge (mm)
a: shear span (mm)

D: height of section (mm)

We can then use Expression (7) to calculate the displacement due to rotation of the plastic hinge section by setting the center of rotation at the center of the plastic hinge and using the average curvature in the section, the length of the equivalent plastic hinge, and the shear span.

$$\delta p = \varphi p \cdot Lp \cdot (a - Lp/2) \quad \ldots \quad (7)$$

Where,
δp: displacement due to rotation of the plastic hinge (mm)
φp: average curvature of the plastic hinge section (1/mm)
Lp: length of the equivalent plastic hinge (mm)
a: shear span (mm)

We can obtain the displacement ($\delta 0$) of the skeleton after yielding of the member as the sum of the displacement resulting from rotation of the plastic hinge section (δp) and the displacement (δb) of the skeleton in the non-plastic-hinge section.

c) Displacement of skeleton away from plastic hinge
We calculate the displacement of the skeleton at locations other than the plastic hinge at the ultimate displacement by dividing the member into 100 cross sections in the axial direction and integrating the curvature of each cross section. In calculating these curvature values, we regard the total cross section as effective when cracking does not occur in the calculation, but neglect the concrete on the tensile side when cracking occurs, just as in the calculation of yield displacement. It is determined that cracking occurs when the tensile stress at the tensile end reaches the flexural strength considering the size of members [5].

d) Displacement due to rotation of plastic hinge
We calculate the displacement (δup) of the plastic hinge section at the ultimate displacement by subtracting the displacement (δub) of the skeleton away from the plastic hinge and the rotational displacement ($\delta u1$) arising from pull-out of the axial reinforcement (both at the ultimate displacement) from the measured ultimate displacement ($\delta utest$). We then calculate back the average curvature of the plastic hinge at the ultimate displacement using the Expression (7) and the value of δup obtained above; this is taken to be the measured average curvature ($\varphi putest$) of the plastic hinge at the ultimate displacement.

In discussing a method for calculating the average curvature of the plastic hinge section, we first consider the effect of the number of cycles of repeated loading. Table 4 gives the values of $\varphi putest$ for specimens subjected to one cycle of reversed cyclic loading under loading pattern B and those subjected to three cycles of loading under loading pattern A at different displacements but with the same values of web reinforcement ratio and other parameters. Also given is the ratio of one-cycle to three-cycle values of $\varphi putest$. The table illustrates that the average curvature of specimens that underwent three-cycle loading tends to be smaller than that of those that underwent one-cycle loading, with the average ratio of the two being 0.87. In calculating average curvature, we followed past research [10] and basically adopted three-cycle loading with different displacements, correcting the value of $\varphi putest$ for specimens subjected to

Table 4 Comparison of values of measured average curvature of plastic hinge with different loading cycles and displacements

ϕputest (1/mm)				Ratio
Three-cycle loading		One-cycle loading		Three-cycle/one-cycle
R3	0.000159	A1	0.000196	0.81
A7	0.000187	K1	0.000202	0.93
R4	0.000174	R1	0.000201	0.87
				Average ratio 0.87

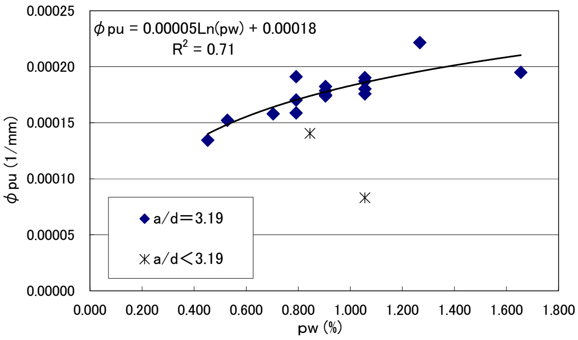

Fig. 15 Relationship between φpu and pw

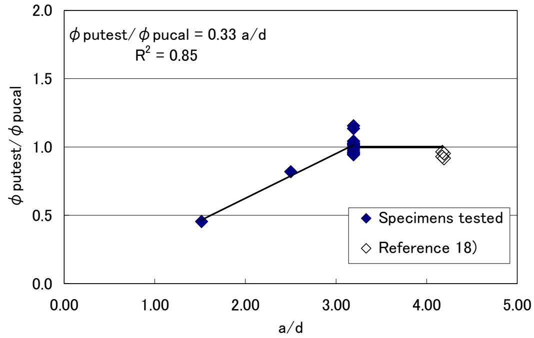

Fig. 16 Effect of different values of a/d on φpu

one-cycle loading by the factor 0.87 obtained above. This correction factor of 0.87 is approximately in agreement with test results obtained by Machida et al. [17] who studied the effect of the cyclic loading on the plastic deformation of RC columns.

Figure 15 shows the relationship between average curvature of the plastic hinge and the web reinforcement ratio (pw). Here, the average curvature tends to increase as the web reinforcement ratio increases in the plastic hinge region. The test results for specimens with a shear span ratio of 3.19 yield Expression (8).

$$\varphi pu = 0.00005Ln(pw) + 0.00018 \quad \ldots \quad (8)$$

Where,
φpu: average curvature of plastic hinge at ultimate displacement (1/mm)
pw: web reinforcement ratio (%)
Ln: $\log_e$

In Fig. 16, the X-axis represents the shear span ratio and the Y-axis the ratio of measured value ofaverage curvature of the plastic hinge at the ultimate displacement (φputest) to the value calculated using Expression (8) (φpucal). Also shown in this figure are data reported by Hoshikuma et al. [18], which cover values of shear span ratio that are higher than those used in this study. The average curvature of the plastic hinge at the ultimate displacement as calculated by Expression (8) approximates to the measured value when the shear span ratio is greater than 3.19, which is the value used in our study. On the other hand, specimens A11 (shear span ratio: 2.50) and A10 (1.52) indicate that the ratio of average measured to calculated curvature tends to fall as the shear span ratio decreases.

When the shear span ratio is less than about 3, the stress distribution approaches that of a deep beam, and the concrete under compressive stress may suffer damage earlier as a result of the changed stress distribution. As the shear span ratio decreases, therefore, it is thought that the ultimate displacement and the maximum displacement required to maintain the maximum load (the maximum load/displacement) become smaller, according to the corrected expression of 0.33a/d as obtained from the test data. Since the amount of data is small, however, we show corrected values for the specimens with shear span ratios of 2.50 and 1.52 for reference in the figures referred to in the following discussion.

Figure 17 shows the relation between the measured average curvature (φputest) of the plastic hinge at the ultimate displacement divided by the calculated value (φpucal) and the tensile reinforcement ratio (pt). This figure shows that there is no particular correlation when the tensile reinforcement ratio is from 0.440 to 0.995%.

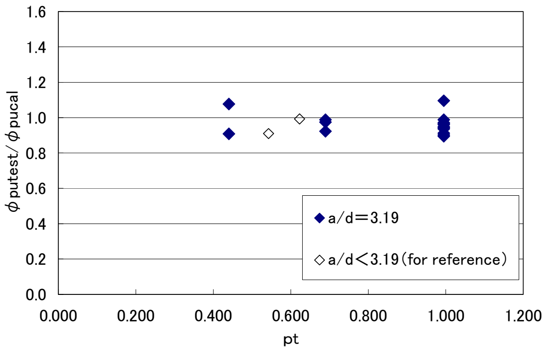

Fig. 17 Effect of different values of pt on φpu

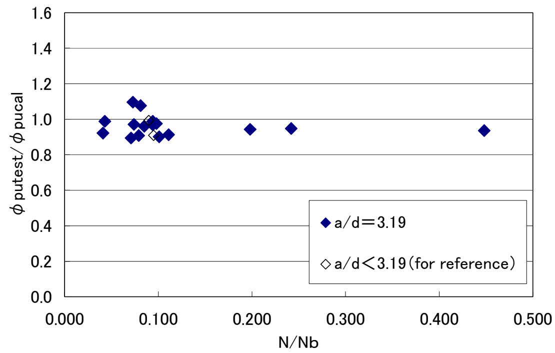

Fig. 18 Effect of different values of N/Nb on φpu

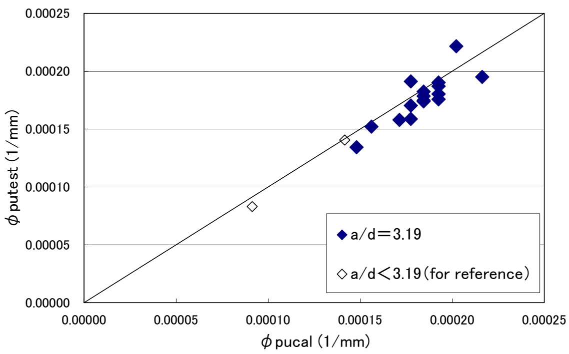

Fig. 19 Comparison of φputest and φpucal

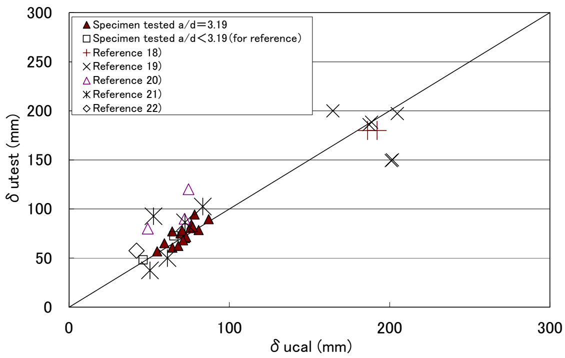

Fig. 20 Comparison of δutest and δucal

To discuss the effect of axial compressive stress, we show the relationship between φputest divided by φpucal and the balanced axial force (N/Nb) in Fig. 18, where N is the working axial force and Nb is the balanced axial force, meaning the acting axial force calculated when the concrete strain at the compression edge reaches 0.0035 simultaneous with yielding of the outermost axial reinforcement due to tension. Figure 18 indicates that there is no particular correlation in the range ($0.041 \leqq N/Nb \leqq 0.448$) as tested in this study.

Based on the discussion above, we obtain Expression (8) for calculating the average curvature (φpu) of the plastic hinge when the RC column is at the ultimate displacement. Figure 19 compares the measured values (φputest) and calculated values (φpucal). The average of the ratio φputest/φpucal is 0.962 and the coefficient of variation is 5.4%. This means that Expression (8) reflects the test results to comparatively high precision.

We can calculate the displacement (δup) due to rotation of the plastic hinge at the ultimate displacement using Expression (7) and the average curvature (φpu) of the plastic hinge at the ultimate displacement as given by Expression (8).

e) Comparison of calculated and measured values of ultimate displacement
Figure 20 compares the measured value (δutest) of ultimate displacement and the value (δucal) calculated as the sum of rotational displacement arising from pull-out of the axial reinforcement, rotational displacement due to rotation of the plastic hinge, and displacement of the skeleton away from the plastic hinge (all at the ultimate displacement) by the methods explained in Sections 4.(3) a), 4.(3) c), and 4.(3) d). The evaluation method adopted in this study was verified for data at a strength ratio of about

2.0 taken from references [18], [19], [20], [21] and [22] and appropriate results were obtained, as shown in Fig. 20. Other parameters used in the discussion were: reinforcement ratio 0.10 to 1.66%; shear span ratio 1.52 to 5.56; tensile reinforcement ratio 0.29 to 1.07%; and balanced axial force ratio 0 to 0.448.

(4) Maximum load/displacement (point M)

In the same way as for ultimate displacement, we obtain the maximum load/displacement (δm) as the sum of the rotational displacement (δm1) arising from pull-out of the axial reinforcement and the displacement (δm0) of the skeleton, both at the ultimate displacement, where δm0 is the sum of the displacement (δmp) due to the rotation of the plastic hinge and the displacement of the skeleton away from the plastic hinge, both at the maximum load/displacement.

a) Rotational displacement arising from pull-out of axial reinforcement
In the same way as in Section 4.(3) a), we calculate the pull-out of reinforcement from the footing at the maximum load/displacement using expressions (3) to (5). By substituting this value into Expression (2), we can calculate the rotational displacement (δm1) arising from pull-out of the axial reinforcement of the RC column at the maximum load/displacement.

b) Displacement of skeleton away from the plastic hinge
In the same way as for ultimate displacement, we calculate the displacement (δub) of the skeleton away from the plastic hinge at maximum load/displacement by dividing the member into 100 cross sections in the axial direction and integrating the curvature of each.

c) Displacement due to rotation of plastic hinge
Table 5 shows the measured average curvature (φpmtest) of the plastic hinge at the maximum load/displacement for specimens subjected to one cycle of reversed cyclic loading (loading pattern B) and for specimens subjected to three cycles of reversed cyclic loading (loading pattern A) at different displacements but with the same values of web reinforcement ratio and all other parameters. The ratio of the one-cycle to three-cycle values is used to investigate the effect of number of loading cycles in discussing a method of calculating the displacement (δmp) due to rotation of the plastic hinge at the maximum load/displacement. By applying the same method as used for the ultimate displacement, we calculate the value of φpmtest using Expression (7) by subtracting the displacement (δmb) of the skeleton in the non-plastic-hinge section and the rotational displacement (δm1) due to the pull-out of axial reinforcement, both at the maximum load/displacement, from the measured maximum load/displacement (δmtest). Table 5 shows that the average curvature tends to decrease as the number of loading cycles increases at different displacements. The ratio of the average curvature of specimens subjected to one cycle of loading to that of specimens subjected to three cycles of loading is 0.87, which is the same as that at the ultimate displacement. We use this value to correct the value of φpmtest for the specimens subjected to one cycle of loading.

Table 5 Comparison of values of measured average curvature of plastic hinge with different loading cycles at the maximum load/displacement

φpmtest (1/mm)				Ratio
Three-cycle loading		One-cycle loading		Three-cycle/one-cycle
R3	0.000132	A1	0.000163	0.81
A7	0.000127	K1	0.000155	0.82
R4	0.000155	R1	0.000160	0.97
				Average ratio 0.87

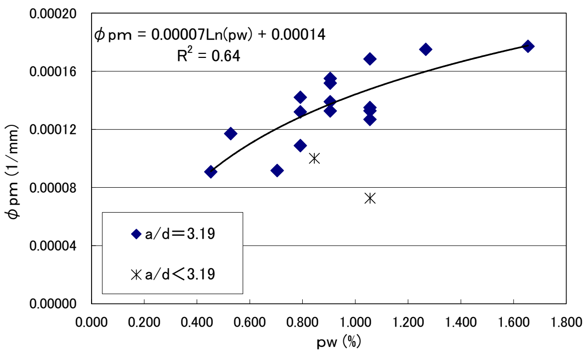

Fig. 21 Relationship between φpm and pw

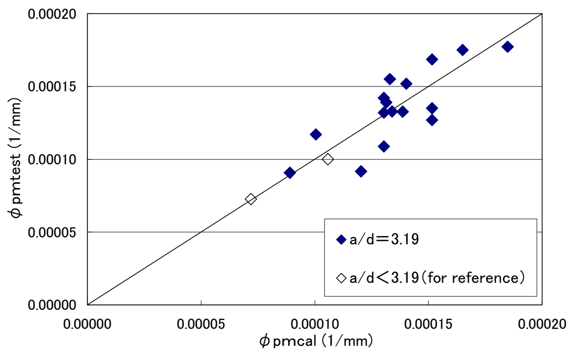

Fig. 22 Comparison of φpmtest and φpmcal

Figure 21 shows the relationship between web reinforcement ratio (pw) and average curvature of the plastic hinge at maximum load/displacement. From the test results for specimens with a shear span ratio of 3.19 in Fig. 21, we obtain Expression (9).

$$\varphi pm = 0.00007Ln(pw) + 0.00014 \quad \ldots \quad (9)$$

Where,
φpm: average curvature of plastic hinge at maximum load/displacement (1/mm)
pw: web reinforcement ratio

Since the average curvature of specimens with shear span ratios of 2.50 and 1.52 is similar to that at the ultimate displacement, we correct the calculated average curvature of the plastic hinge at the maximum load/displacement by multiplying by 0.33a/d. This corrected value is shown in the figures referred to in the discussion that follows.

Figure 22 shows the relationship between the average plastic hinge curvature value (φpmcal) calculated using Expression (9) and the measured value (φpmtest) at maximum load/displacement. The average and the coefficient of variation of φpmtest/φpmcal are 0.994 and 8.9%, respectively. This demonstrates that the proposed expression appropriately reflects the measured values.

The displacement (δmp) due to rotation of the plastic hinge at maximum load/displacement is calculated by substituting the average curvature (φpm) of the plastic hinge at the ultimate load/displacement (as obtained using expression (9)) into Expression (7).

d) Comparison of calculated and measured values of maximum load/displacement

Figure 23 compares the measured value (δmtest) of maximum load/displacement and the value (δmcal) calculated as the sum of the rotational displacement arising from pull-out of the axial reinforcement, the rotational displacement due to rotation of the plastic hinge, and the displacement of the skeleton away from the plastic hinge. All values are at the maximum load/displacement, and the methods given in Sections 4.(4) a), 4.(4) b), and 4.(4) c) are used. Also plotted are data from past research [19]. These results prove that this

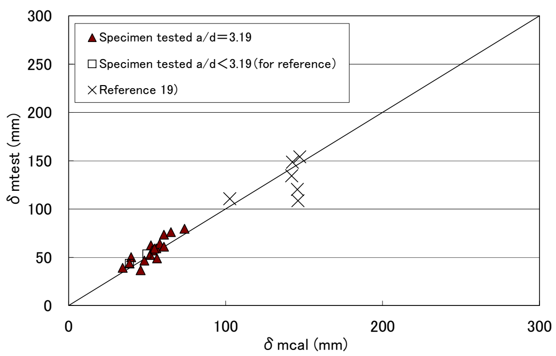

Fig. 23 Comparison of δmtest and δmcal

method of evaluating the deformation capacity of RC columns is appropriate.

5. Summary

To establish a method of quantitatively evaluating the deformation capacity of RC columns in the region of large deformation and at a member ductility factor of about 10, reversed cyclic loading tests were carried out on RC specimens in the parameter ranges given below. Previously reported data and the results of these tests were collated and used as the basis for discussion.
Shear span, a: 1,000 to 9,600 mm
Height of cross section, D: 320 to 2,400 mm
Web reinforcement ratio, pw: 0.10 to 1.66%
Shear span ratio, a/d: 1.52 to 5.56
Ratio of balanced axial force, N/Nb: 0 to 0.448
Tensile reinforcement ratio, pt: 0.29 to 1.07%
Strength ratio, Vyd/Vmu: 1.55 to 3.94
Ratio of reinforcement diameter to cross section, φ/B: 0.011 to 0.048
Shear span ratios lower than 3.19 are outside the applicability of the expressions used to calculate φpu and φpm.
The results of the investigation can be summarized as follows.

(1) The envelope of the load-displacement curve tends to show that the load remains approximately equal to the maximum load after the maximum is reached and until about 80% of the ultimate displacement.

(2) The region where damage is concentrated at the foot of the member after yielding is regarded as a plastic hinge of equivalent length, Lp, and a method of calculating this length is proposed:

$$Lp = 52 \cdot a - 0.6 \cdot D$$

However, $Lp \leqq D$
where,
Lp: length of equivalent plastic hinge (mm)
a: shear span ratio (mm)
D: height of cross section (mm)

(3) A method is proposed for calculating the ultimate displacement δu.

$$\delta u = \delta u0 + \delta u1 = \delta up + \delta ub + \delta u1$$

Where,
δu0: displacement of skeleton at ultimate displacement (mm)
δup: displacement arising from rotation of the plastic hinge at the ultimate displacement (mm)
δub: displacement of the skeleton away from the plastic hinge at the ultimate displacement (mm)
δu1: rotational displacement arising from pull-out of axial reinforcement at the ultimate displacement (mm)
The displacement δup of the plastic hinge at the ultimate displacement can be calculated using the following expression by treating the center of the plastic hinge as the center of rotation:

$$\delta up = \varphi pu \cdot Lp \cdot (a - Lp/2)$$

Where,
δup: displacement arising from rotation of the plastic hinge at the ultimate displacement (mm)
φpu: average curvature of the plastic hinge at the ultimate displacement (1/mm)
Lp: length of the equivalent plastic hinge (mm)
a: shear span (mm)
The average curvature φpu of the equivalent plastic hinge at the ultimate displacement can be calculated using the following expression:

$\varphi pu = (0.00005Ln(pw) + 0.00018)$
However, $0.10 \leqq pw \leqq 1.66$ and $a/d \geqq 3.19$
where,
pw: web reinforcement ratio (%)
a/d: shear span ratio

(4) A method is proposed for calculating the maximum load/displacement δm.
$\delta m = \delta m0 + \delta m1 = \delta mp + \delta mb + \delta m1$
Where,
δm0: displacement of the skeleton at the maximum load/displacement (mm)
δmp: displacement arising from rotation of the plastic hinge at the ultimate displacement (mm)
δmb: displacement of the skeleton away from the plastic hinge at the ultimate displacement (mm)
δm1: rotational displacement arising from pull-out of axial reinforcement at the ultimate displacement (mm)
The displacement arising from rotation of the plastic hinge at the maximum load/displacement is calculated using the following expression:
$\delta mp = \varphi pm \cdot Lp \cdot (a - Lp/2)$
Where,
δmp: displacement arising from rotation of the plastic hinge at the ultimate displacement (mm)
φpm: average curvature of the plastic hinge at the maximum load/displacement (1/mm)
Lp: length of equivalent plastic hinge (mm)
a: shear span (mm)
The average curvature φpm of the equivalent plastic hinge at the ultimate displacement can be obtained with the following expression:
$\varphi pm = (0.00007Ln(pw) + 0.00014)$
However, $0.10 \leqq pw \leqq 1.66$ and $a/d \geqq 3.19$
where,
pw: web reinforcement ratio (%)
a/d: shear span ratio

References

[1] Japan Society of Civil Engineers, Standard Specifications for Concrete Structures (seismic design), 1996
[2] Railway Technical Research Institute, Standard Specifications for Seismic Design of Structures for Railways, 1999 (in Japanese)
[3] Ishibashi, T., Tsuyoshi, T., Kobayashi, K., and Kobayashi, M., "An Experimental Study on Damage Levels and Repairing effects of Reinforced Concrete Columns subjected to ReversedCyclic Loading with Large Deformations", Proc. of JSCE, No.648/V-47, pp.55-69, 2000 (in Japanese)
[4] Ishibashi, T., Kobayashi, K., and Umihara, T., "Study on Quantitative Evaluation of Pull-Out of Longitudinal Bar from Footing of RC Piers Under Cyclic Loading in Large Deformation Range", Proc. of JSCE, No.648/V-47, pp.43-54, 2000 (in Japanese)
[5] Railway Technical Research Institute, Standard Specifications for Design of Concrete Structures for Railways, 1992 (in Japanese)
[6] Niwa, J., Yamada, K., Yokozawa, K., and Okamura, H., "Revaluation of the Equation for Shear Strength of Reinforced Concrete Beams without Web Reinforcement", Proc. of JSCE, No.372/V-5, pp.167-176, 1986 (in Japanese)
[7] Ishibashi, T., Matsuda, Y., and Saito, K., "Proposed Design Method for the Shear Strength of Reinforced Concrete Footings with Few Piles", Proc. of JSCE, No.337/V-5, pp.197-204, 1983 (in Japanese)
[8] Japan Concrete Institute, Symposium Committee Report Regarding the "Situation of the Deterioration of Plasticity Area by Cyclic Loading", pp108, 1998 (in Japanese)
[9] Yagishita, F., Tanaka, H., and Park, R., "Cyclic Behavior of Reinforced Concrete

Columns with Interlocking Spirals", Proc. of JSCE, No.662/V-49, pp.91-103, 2000 (in Japanese)
[10] Ishibashi, T., and Yoshino, S., "Study on Deformation Capacity of Reinforced Concrete Bridge Piers in Earthquakes", Proc. of JSCE, No.390/V-8, pp.57-66, 1988 (in Japanese)
[11] Shima, H., Chou, L., and Okamura, H., "Micro and Macro Models for Bond in Reinforced Concrete", Journal of the Faculty of Engineering, The University of Tokyo (B), Vol.XXXIX, No.2,pp.133～194, 1987.
[12] Shima, H., Sinohara, K., and Morioka, H., "Influence of Reinforcing Bars Spacing on Pull-out of Reinforcing Bars Anchored in Footing", Proc. of JCI Symposium concerning "Ductility and Arrangements of Reinforcing Bars", pp.109-114, 1990 (in Japanese)
[13] Japan Society of Civil Engineers, Seismic Technology of Concrete Structure - Present Condition and Future View, Concrete Engineering Series, Vol.20, 1997
[14] Kosa, K., Kobayashi, K., Murayama, Y., and Yosizawa, Y., "Experimental Study on Reversed Load-Displacement Behavior pf RC Pier by Large Scale Model Tests", Proc. of JSCE, No.538/V-31, pp.47-56, 1996 (in Japanese)
[15] Hoshikuma, J., Unjoh, S., and Nagaya, K., "Size Effect on Inelastic Behavior of Reinforced Concrete Columns Subjected to Cyclic Loading", Proc. of JSCE, No.669/V-50, pp.215-232, 2001 (in Japanese)
[16] Public Works Research Institute, "Study on Length of Plastic Hinge in Reinforced Concrete Bridge Pier by Buckling Analysis of Axial Reinforcement", Technical Memorandum of PWRI, Vol.3748, 2000 (in Japanese)
[17] Machida, A., Mutsuyoshi, H., and Toyoda, K., "Evaluation of Ductility of Reinforced Concrete Members", Proc. of JSCE, No.378/V-6, pp.203-212, 1987 (in Japanese)
[18] Hoshikuma, J., Unjoh, S., Nagaya, K., and Ikeda, H., "Flexural Behavior of Reinforced Concrete Bridge Columns Based on Cyclic Loading Tests on Large-scale Models", Proc. of The 10th Japan Earthquake Engineering Symposium, pp.2123-2128, 1998 (in Japanese)
[19] Tanaka, H., Okamoto, M., Takiguchi, M., and Sato, T., "An Experimental Study on the Ductility and Damage Level of RC Columns", Proc. of JCI, Vol.20, No.3, pp.1045-1050, 1998 (in Japanese)
[20] Hoshikuma, J., Unjoh, S., Kawashima, K., and Nagaya, K., "A Ductility Evaluation of Flexural Reinforced Concrete Columns Based on Loading History and Plastic Curvature", Journal of Structural Engineering, Vol.44A, pp.877-888, 1998 (in Japanese)
[21] Kawashima, K., Hasegawa, K., Nagashima, H., Koyama, T., and Yoshisa, T., "Study on Development of Designs for Ultimate Lateral Strength under Earthquake of Reinforced Concrete Bridge Piers", Journal of PWRI, Vol.190, 1993 (in Japanese)
[22] Iketani, K., Yoshikawa, H., Miyagi, T., and Hattori, H., "Evaluation of Failure Mode and Ductility of Reinforced Concrete Columns", Proc. of JCI, Vol.20, No.3, pp.259-264, 1998 (in Japanese)